Available online at www.sciencedirect.com

ScienceDirect

Procedia CIRP 58 (2017) 91 – 96

www.elsevier.com/locate/procedia

16th CIRP Conference on Modelling of Machining Operations

Cutting simulation with consideration of the material hardening in the shear zone of AISI1045

E. Uhlmann[a], S. Henze[a]*, K. Brömmelhoff[b], W. Reimers[b]

[a]*Institute for Machine Tools and Factory Management, Technische Universität Berlin, Pascalstraße 8-9, 10587 Berlin, Germany*
[b]*Institute for Materials Science and Technology-Metallic Materials, Technische Universität Berlin, Ernst-Reuter-Platz 1, 10587 Berlin, Germany*

* Corresponding author. *E-mail address: henze@iwf.tu-berlin.de*

Abstract

By the use of high energy synchrotron X-ray diffraction it was possible to determine the stress state in the chip formation zone during orthogonal cutting of AISI1045. The analysis of the diffractograms showed a hardening of the material during the movement through the shear zone. For this reason nano indentation experiments on prepared chips have been carried out. With these experiments, the material hardening has been confirmed. The nano indentation experiments were reproduced by FEM simulations and it was possible to determine flow curves of the hardened material above the shear zone based on existing flow curves of AISI1045. Thus, cutting simulations have been carried out, which considered the material hardening in the shear zone. The simulation results were then compared with the results of the in-situ strain measurements.

Peer-review under responsibility of the scientific committee of The 16th CIRP Conference on Modelling of Machining Operations

Keywords: Chip; Simulation; Nano indentation; Hardening; Cutting

1. Introduction

For the simulation of cutting processes material and friction models are needed [1]. Flow curves are used for the preparation of the material model, which describe the flow properties of the workpiece material. In general the flow curves are determined by tensile or compression tests. The cutting process is characterized by a wide range of temperature, strain and strain rate [1]. Thus the flow curves have to be determined by tests with different temperatures and strain rates. Especially the high temperatures, which can be reached during cutting processes, are challenging for the determination of flow curves. Most commercial software applications for the simulation of machining processes provide material databases which can be used. However the quality of the material models of the various databases differs. Additionally the range of values is often restricted. Thus a limited temperature range can often only be covered.

The nano indentation method from OLIVER AND PHARR was introduced in 1992 for the determination of hardness and the elastic modulus on a small scale [2]. The nano indenter is made of diamond and is pressed to the surface with increasing load until a specific maximum force is reached. Hardness and the elastic modulus can be obtained by the force-displacement diagram. The benefit of the method introduced by OLIVER AND PHARR is the fact that there is no need to image the hardness impression [3]. In particular the measurement of thin films is the main field of application for nano indentation. In addition it is possible to obtain flow curves by nano indentation experiments in combination with FEM simulations. BOBZIN ET AL. have used this method for the nickel-base alloy Inconel 625 and the stainless steel AISI304 [4]. The small size of the nano indenters of just a few hundred nanometres gives the possibility to carry out nano indentation tests on small specimens. Thus it is possible to determine hardness, elastic modulus and also flow curves on the chip roots of cutting experiments.

Peer-review under responsibility of the scientific committee of The 16th CIRP Conference on Modelling of Machining Operations
doi:10.1016/j.procir.2017.03.199

Nomenclature

A	projected area of the nano indentation impress
d_e	penetration depth
F_{NI}	Nano indentation force
h	undeformed chip thickness
H	Hardness determined by nano indentation
l_c	contact length between chip and rake face
l_e	edge length of an element in the FE-Simulation
m	shear friction coefficient
r_β	cutting edge radius
t	exposure time
t_h	holding time
v_c	cutting speed
φ	plastic strain
γ	rake angle
μ	Coulomb friction coefficient

By the use of high energy synchrotron X-ray diffraction it was possible to determine the strain state and thus the stress state in the chip formation zone during orthogonal cutting [5]. A special experimental setup for measurements at the PETRA III storage ring at DESY, Hamburg was developed for this purpose [6]. With this setup it was possible to position an X-ray beam on a sample of AISI1045 during an orthogonal cut. The beam had a size of 20 µm x 20 µm. Different measuring positions in the chip formation zone have been defined in order to gain detailed information regarding the stress state in the chip formation zone. The setup of the cutting experiment was therefore placed between the X-ray beam source and the 2D detector (type MAR345, Marresearch, Norderstedt, Germany) which captured the diffraction patterns. The diffraction experiments were carried out according to the Debye-Scherrer method [7].

The cutting speed is limited to $v_c = 3$ mm/min. This is due to the long exposure time of the detector of t = 30 s and the need for a very stiff cutting setup to avoid a displacement of the measuring position during the in-situ experiment. The used cutting inserts are made of cemented carbide (grade IC20, ISCAR Germany GmbH, Ettlingen) and have the ISO-geometry SPUN 120304 with a rake angle of $\gamma = 10°$ and a cutting edge radius of $r_\beta = 6$ µm. A more detailed description of the experimental setup is described by UHLMANN ET AL. [6].

Through the analysis of the data obtained by the in-situ strain measurements, it was possible to develop a material model for the cutting simulation of AISI1045. The simulations with this model showed a good qualitative and partially quantitative accordance in comparison to the experimentally determined data. Certain deviations between simulation and experiments could be determined for the forces, the shear angles and partially the stresses. An investigation of the experimentally determined stress state in the chip formation zone resulted in new findings with regard to the shear angle model by OPITZ AND HUCKS [6, 8].

The analysis of the chip roots showed evidence that built-up edges (BUE) appeared during the in-situ strain measurements for certain cutting parameters [9]. This is a common phenomenon for the low cutting speed of $v_c = 3$ mm/min. Tools with a cutting edge radius of $r_\beta = 30$ µm und $r_\beta = 60$ µm showed remains of a BUE in the analysis of the chip roots. By analysing the BUEs at the chip roots of the in-situ experiments, it was possible to determine the geometry of the BUE. Using the obtained data a simulation model which represents the BUE could be established with two versions of the BUE: a solid one as part of the rigid tool and an elastic one in front of the tool. Using FEM cutting simulations with and without BUEs, it was possible to show the influence of a BUE on the chip formation and the stress state in the chip formation zone [9].

2. Material hardening in the shear zone

Various findings regarding the chip formation during the cutting process could be gained by the evaluation of the data obtained by the in-situ strain measurements. The analyses of the stresses resulted in new findings on the processes in the chip formation zone. It could be shown that the simplifying assumption of a free chip flow of the shear angle model of OPITZ AND HUCKS [8] is not permissible [6].

The analysis of the diffractograms showed that the material is exposed to significant microstructural modifications while passing the shear zone. A reorientation of the crystallites occurs and preferred orientations establish [10]. In addition, a material hardening in the shear zone could be observed. Thus the material in the chip above the shear zone is harder than the initial material. Until now this material hardening was not considered by the simulations. However, it can be assumed that this has a considerable influence on the chip formation process and thus, the cutting forces, the chip formation and finally the stress and the strain state. An implementation of the different material properties below and above the shear zone in the simulations should thus lead to a better quality of the simulation.

3. Nano indentation and determination of flow curves

3.1. Nano indentation experiments

Nano indentation experiments were carried out on the chip roots obtained by the in-situ strain measurements. The aim was to verify the material hardening and to determine the flow curves in the hardened material. The nano indentation tests were carried out by the Institute of Mechanics of the Technische Universität Berlin. Usually nano indentation tests are used to qualify the mechanical properties of thin films. Due to the limited spatial conditions on the chip roots, the tests are also suitable to determine the hardness beneath and above the shear plane. For this purpose a diamond indenter with a Berkovich geometry was used. The indenter is pressed with a maximum force of $F_{NI} = 500$ mN on the specimen and generates a triangular indentation. The penetration depth varies between $d_e = 150$ nm and $d_e = 2000$ nm, depending on the tested material. The hardness can be calculated by equation 1 as the quotient between the indentation Force F_{NI} and the projected area A of the indentation.

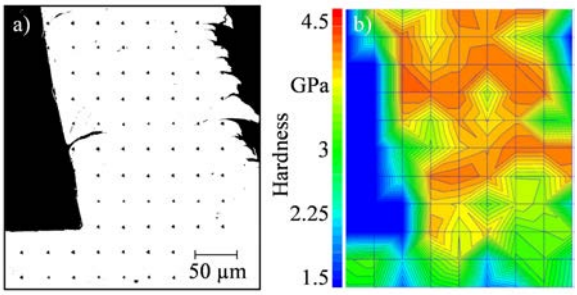

Fig. 1. (a) Mapping of the nano indentation on a chip root; (b) measured hardness values (γ = 10°, h = 60 µm).

$$H = \frac{F_{NI}}{A} \quad (1)$$

Figure 1a shows a chip root (γ = 10°, h = 60 µm) on which nano indentation tests have been carried out. On an area of 300 µm x 240 µm, 99 indentations were made. The maximal penetration depth was d_e = 600 nm. The indentation process is force-stroke controlled. The indenter is pressed with a linear increasing force until a defined maximum force is achieved. Afterwards the constant load is held for a holding time of t_h = 30 s. Finally the force decreases linearly. Thus, force-displacement diagrams have been generated for each indentation point on the chip root. According to equation 1 the hardness values for the 99 indentations were calculated. Figure 1b shows the mapping of the hardness on the chip root given in figure 1a. It can clearly be seen that the hardness above the shear zone is higher.

3.2. Simulation of the nano indentation and determination of the flow curves

The nano indentation tests were depicted by a FEM-simulation carried out with the Software DEFORM 2D v11.0, Scientific Forming Technologies, Ohio, USA. The three-dimensional Berkovich-geometry was transformed to a axisymmetric 2D-modell according to the method of BOUZAKIS ET AL. [11]. Aim of the simulation was to depict the force-displacement behaviour of the nano indentation experiments. Due to the inhomogeneity of the hardness values caused by the ferrite-perlite structure the reference was averaged over the nano indentation points in the chip above the shear zone. The procedure corresponds to the method of BOBZIN ET AL. [4]. The indenter is considered as a rigid body. The material model of the workpiece material is based on the model that was used for the simulations within the previous investigations [6, 9]. The flow curves used in this model were obtained by compression tests with a Rastegaev geometry with different strain rates [6, 12]. A more detailed description of the material model is described by UHLMANN ET AL. [6]. The flow curves were integrated as mathematical functions in the subroutines of DEFORM. In order to depict the material hardening in the shear zone the flow curves were modified

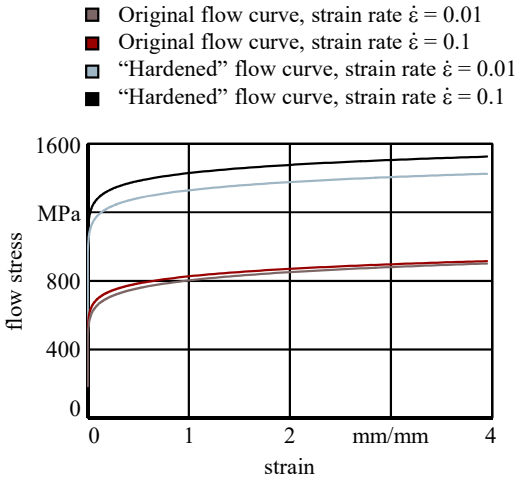

Fig. 2. Flow curves.

by an offset. By an iterative procedure with a variation of the offsets, it was possible to determine flow curves that are able to depict the force-displacement behaviour of the nano indentation above the shear zone in an adequate manner. Figure 2 shows the flow curves of the original material and of the hardened material above the shear zone.

4. Simulation model

By the determination of the flow curves beneath and above the shear zone it was possible to prepare a cutting simulation model with consideration of the material hardening in the shear zone. For this purpose the flow curves were integrated as mathematical functions in the subroutines of DEFORM. The detection of the shear zone was realized by the evaluation of the strain rates as shown in figure 3. The straight $\overline{P_1P_2}$ represents the shear plane and thus the border between the original and the higher flow curves. The point P1 complies with the tool tip and is defined as the point of origin. In this case a cutting edge radius of r_β = 6 µm was used for the experiments and thus for the simulation-model. In consequence the cutting edge radius has a minor influence on the position of P1. For higher cutting edge radii the definition of the point P1 has to be made with an analysis of the strain rates in front of the cutting edge. The highest strain rates occur in the shear plane. Thus the point P2 is defined as the point with the highest strain rates. Whereby y > h applies for the y coordinate of the point. By the use of this definition of the straight $\overline{P_1P_2}$ it is ensured that the border between the original and the hardened material is also defined for a varying shear angle.

The finite element model was depicted in DEFORM 2D. The workpiece, made of AISI1045, consists of about 8,000 elements. Due to remeshing procedures the exact amount varies. In the area around the cutting edge a finer mesh with an element edge length of l_E = 3 µm is defined. A hybrid friction model with a Coulomb friction coefficient of µ = 0.5 and a shear friction coefficient of m = 0.577 was used. In the

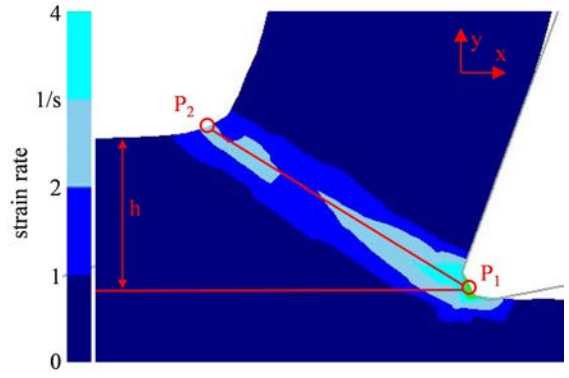

Fig. 3. Detection of the shear zone.

previous works this friction model showed the best correlations compared to the experimental results [6, 9]. A cutting speed of $v_c = 3$ mm/min, a rake angle of $\gamma = 10°$ and an undeformed chip thickness of $h = 60$ µm were used for the simulation. These cutting parameters correspond to the parameters used in the in-situ strain measurements.

5. Results

Using the described simulation model cutting simulations without and with consideration of the material hardening were carried out in the software DEFORM 2D v11.0. Due to the in-situ strain measurements it is possible to compare the stress state in the shear zone additionally to the shear angles and the cutting forces.

5.1. Shear angles

In table 1 the shear angles of the simulations with and without the material hardening and those measured on the chip roots are given. The integration of the material hardening leads to a better correlation between the simulation and the experiments. The measured shear angles were between $\Phi = 16°$ and $\Phi = 18°$. Simulations without consideration of the material hardening clearly overestimate the shear angle with a value of $\Phi = 24°$. Due to the implementation of the material hardening the shear angle is reduced to $\Phi = 15°$. This is slightly lower than the shear angles from the experiment. By the consideration of the material hardening the correlation of the shear angles between experiment and simulation could be improved. The contact between chip and rake face is characterized by the contact length l_c. Compared to the simulations, the contact length in the experiments is between two and three times as long. Thus the bend of the chip is higher in the simulations. The smaller contact area between chip and rake face has an influence on the cutting forces, which will be discussed later.

Table 1. Shear angles and contact lengths

h = 60 µm γ = 10°	Shear angle Φ	Contact length l_c [µm]
Simulation without material hardening	24°	110 … 120
Simulation with material hardening	15°	145 … 155
Experiments	16° … 18°	300 … 360

5.2. Forces

Table 2 gives the forces that were measured during the in-situ experiments and those received by the simulations. During the previous investigations it could be observed that the simulations underestimate the cutting forces, in particular the passive force F_p [6, 9]. For 2D simulations this effect increases. The implementation of the material hardening in the cutting simulation raises the forces. Thus the cutting force F_c reaches almost the experimental determined value. The passive force F_p is still too low. One reason can be found in the shorter contact lengths (see table 1). The passive forces in the simulation are calculated by the stresses in the contact area between the chip and the rake face and the size of the contact area. Another reason for the deviation of the passive force F_p is the inevitable interference of the elements at the cutting edge. Thus numerical errors occur, which affect the passive forces in particular. Furthermore it was shown before that use of a Coulomb friction model leads into a better correlation of the forces between simulation and experiment [6]. However, a better agreement between the experimental stresses and the stresses from the simulation with the hybrid friction model could be observed. For this reason the hybrid friction model was used for the simulations [6].

Table 2. Cutting and passive forces of the simulations and experiments

h = 60 µm γ = 10°	Cutting Force F_c [N]	Passive Force F_p [N]
Simulation without material hardening	114	20
Simulation with material hardening	131	26
Experiments	144	115

5.3. Stresses

Using the data obtained from the in-situ cutting experiments it is possible to compare the simulations and the experiments regarding the stresses in the shear zone. The results from the experiments, the simulations without and the simulations with consideration of the material hardening are given in figure 4. The simulated stresses were averaged over several points and simulation steps. Thus, the spatially and temporally integrative character of the in-situ strain measurements is taken into account. Additionally, the maximum and minimum values of the simulated stresses within the beam cross-section are represented by scatter bars in the diagrams. The error bars of the experimental results

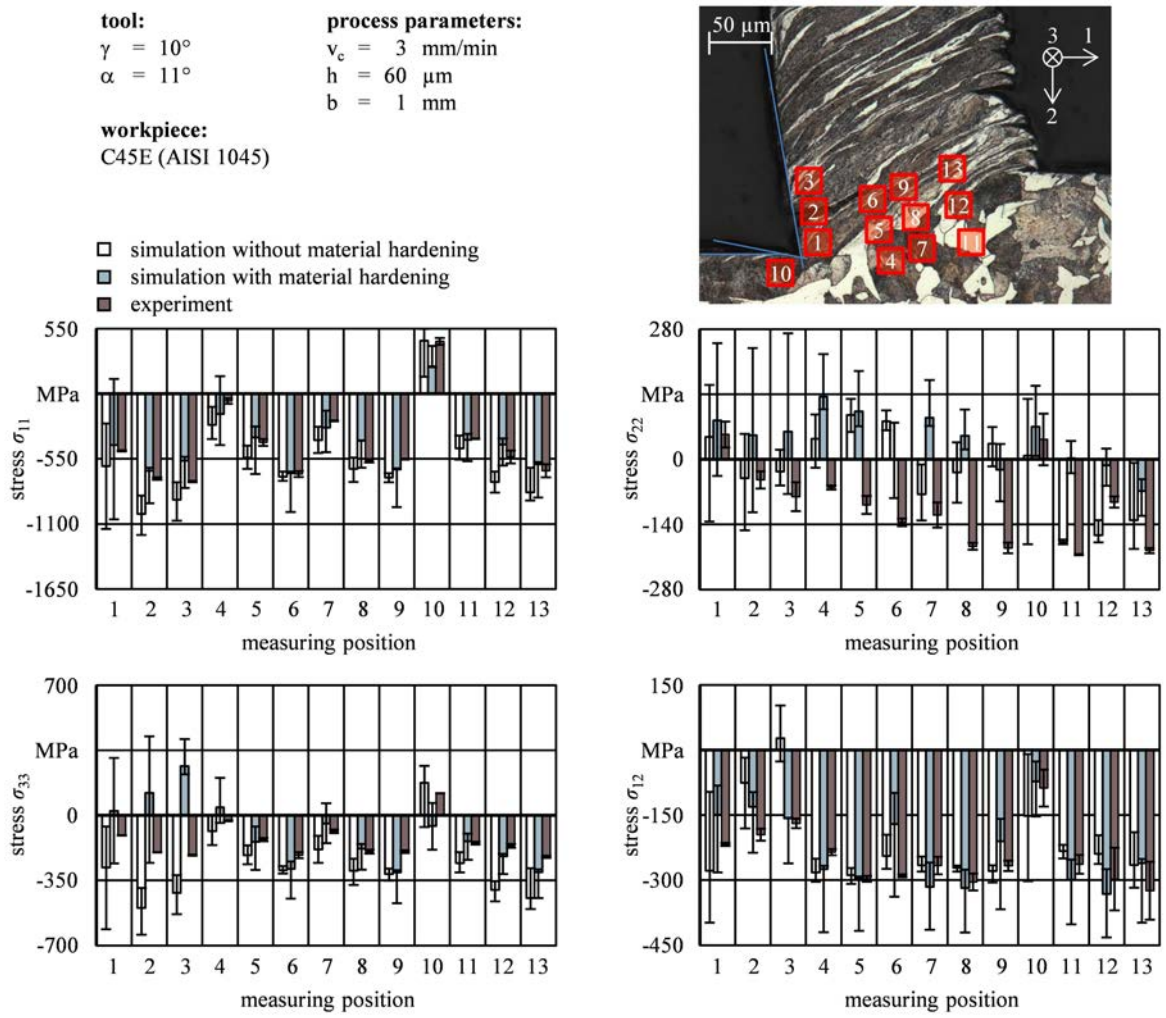

Fig. 4. Stresses obtained by the experiments and the simulations.

represent the deviations between the results from the evaluation of low order and high order reflections.

The comparison shows a good qualitative and quantitative correlation of the simulation without the material hardening and the experiments for the normal stresses σ_{11}. The integration of the material hardening improves the results. On ten out of 13 measuring positions the deviations decrease. Altogether the deviations between experiment and simulation are reduced by about 40 % for the normal stresses σ_{11}. For the shear stresses σ_{12} the simulation without consideration of the material hardening shows a very good correlation with the experiments, with the exception of a small number of measuring positions, for example number 1, 2 and 3. The integration of the material hardening leads to a better accordance on the positions 2 and 3. On the other measuring positions just minimal changes can be observed. Larger differences can be observed at the stresses σ_{22} for both simulations. Earlier investigations showed that the experimental stresses σ_{22} seem to be more accurate [6]. The integration of the material hardening does not lead to a better correlation for the normal stresses in the 2-direction. The experimental stresses σ_{33} were calculated on the basis of the plane strain state out of the stresses σ_{11} and σ_{22}. They show a good qualitative correlation with the stresses determined by the simulations without consideration of the material hardening. The integration of the material hardening leads to change from compressive stresses to tensile for the measuring position 1, 2 and 3 and from tensile to compressive at measuring position 10. For all other positions the correlation between experiment and simulation improves with consideration of the material hardening

In summary, the integration of the material hardening leads to a better correlation of the stresses between simulation and experiment. Especially for the normal stresses σ_{11} and the shear stresses σ_{12} the deviations increase. For the normal stresses σ_{22} the big differences between simulation and

experiment could not be improved by the integration of the material hardening.

6. Conclusions and Outlook

By the use of nano indentation experiments it was possible to verify the assumption of a material hardening in the shear zone during the cutting process. In addition flow curves could be determined for the area above the shear zone by simulations of the nano indentation process using the obtained force-displacement diagrams. The flow curves were integrated in 2D cutting simulations. As a result the correlation between simulation and experiments could be improved for the cutting forces, the shear angles and for the majority of the stresses. The poor accordance for the stresses σ_{22} remains with the integration of the material hardening. Some processes in the chip formation zone are still not taken into account by the simulation. During the movement through the shear zone the grains significantly deforms and get an elongated shape (see figure 4). This morphology of the microstructure may be connected with an anisotropic material behaviour in the chip, which is not depicted by the simulation and could be a reason for the deviations of the stresses σ_{22} between simulation and experiment.

Upcoming investigations should aim to verify the findings for other cutting parameters. During the in-situ strain measurements the rake angle γ, the cutting edge radius r_β and the undeformed chip thickness h have been varied. The comparison with the used parameter set will show if the integration of the material hardening improve the simulation quality for the orthogonal cutting process in general.

One limitation of the in-situ cutting experiments that were carried out is the low cutting speed of $v_c = 3$ mm/min. The specific circumstances of the experimental set up at the storage ring require these cutting speeds. In order to investigate the findings for realistic parameters a new experimental set up has to be investigated.

Acknowledgements

The authors are grateful for the financial support from the Deutsche Forschungsgemeinschaft (DFG) in the project “In-situ Dehnungsmessung bei der Zerspanung mit geometrisch bestimmter Schneide”, and for the granting of beamtime by the Helmholtz-Zentrum Geesthacht. Prof. Dr. W. H. Müller and Arion Juritza from the Institute of Mechanics are acknowledged for the implementation of the nano indentation experiments. Nils Bergström and Martina Elsäßer are acknowledged for the support during the preparation of the simulations and the data evaluation.

References

[1] Mamalis AG, Horváth M, Branis AS, Manolakos DE. Finite element simulation of chip formation in orthogonal metal cutting. J. Mat. Process. Technol. 2001, 110(1): 19-27. DOI 10.1016/S0924-0136(00)00861-X.

[2] Oliver WC and Pharr GM. An improved technique for determining hardness and elastic modulus using load and displacement sensing indentation experiments. J. Mat. Res. 1992; 7(6): 1564–1583. DOI 10.1557/JMR.1992.1564.

[3] Oliver WC and Pharr GM. Measurement of hardness and elastic modulus by instrumented indentation: Advances in understanding and refinements to methodology. J. Mat. Res. 2004; 19(1): 3–20. DOI 10.1557/JMR.2004.19.1.3.

[4] Bobzin K, Bagcivan N, Theiß S, Brignara R, Perne J. .Approach to determine stress strain curves by FEM supported nanoindentation. Mat.-wiss. u. Werkstofftech. 2013; 44(6): 571-576. DOI 10.1002/mawe.201300099.

[5] Uhlmann E, Gerstenberger R, Herter S, Hoghé T, Reimers W, Camin B, Martins RV, Schreyer A, Fischer T. In situ strain measurement in the chip formation zone during orthogonal cutting. Prod Eng Res Dev 2011; 5:1–8. DOI 10.1007/s11740-010-0266-x.

[6] Uhlmann E, Henze S, Gerstenberger R, Brömmelhoff K, Reimers W, Fischer T, Schell N. An extended shear angle model derived from in situ strain measurements during orthogonal cutting. Prod Eng Res Dev 2013; 7: 401-408. DOI 10.1007/s11740-013-0471-5.

[7] He BB. Two-dimensional X-ray diffraction. John Wiley & Sons 2009.

[8] Opitz H, Hucks H. Der Zerspanungsvorgang als Problem der Mohr’schen Gleitflächentheorie für den zwei- und dreiachsigen Spannungszustand. Werkstattstechnik und Maschinenbau 1953; 6: 253-260.

[9] Uhlmann E, Henze S, Brömmelhoff K. Influence of the built-up edge on the stress state in the chip formation zone during orthogonal cutting of AISI1045. Procedia CIRP 31 (2015) 310-315.

[10] Brömmelhoff K, Henze S, Gerstenberger R, Fischer T, Schell N, Uhlmann R, Reimers W. Space resolved microstructural characteristics in the chip formation zone of orthogonal cut C45E steel samples characterized by diffraction experiments. J. Mat. Proc. Tech. 2013, 213 (12): 2211-2216.

[11] Bouzakis K-D, Michailidis N, Erkens G. Thin hard coatings stress-strain curve determination through a FEM supported evaluation of nanoindentation test results. Surface and Coatings Technology 2001; 142-144: 102-109.

[12] Oberländer T. Ermittlung der Fließkurven und der Anisotropie-Eigenschaften metallischer Werkstoffe im Rastegaev-Stauchversuch. Springer, Berlin. 1990.